Saudi Pharmaceutical Journal 31 (2023) 889–903

HOSTED BY

Contents lists available at ScienceDirect

Saudi Pharmaceutical Journal

journal homepage: www.sciencedirect.com

Original article

# Design and dermatokinetic appraisal of lornoxicam-loaded ultrafine self-nanoemulsion hydrogel for the management of inflammation: *In vitro* and *in vivo* studies

Saleh A. Al-Suwayeh, Mohamed M. Badran *, Ghada O. Alhumoud, Ehab I. Taha, Lubna Y. Ashri, Mohsin Kazi

*Department of Pharmaceutics, College of Pharmacy, King Saud University, Riyadh 11451, P.O. Box 2457, Saudi Arabia*

ARTICLE INFO

*Article history:*
Received 31 January 2023
Accepted 3 April 2023
Available online 15 April 2023

*Keywords:*
Lornoxicam
Ultrafine self-nanoemulsion Gel
Skin permeation
Dermatokinetic anti-inflammatory effect

ABSTRACT

The present study aimed to evaluate the impact of ultrafine nanoemulsions on the transdermal delivery of lornoxicam (LOR) for management of the inflammation. The transdermal administration of LORNE could increase the efficacy of LOR with a reduction in side effects. Merging the beneficial properties of ultrafine nanoemulsions and their components (penetration enhancers) can lead to good solubilization, a small droplet size, and more effective LOR carriers. Therefore, this study aims to develop and evaluate the potential use of ultrafine nanoemulsions of LOR (LORNE) to elucidate their skin targeting for the treatment of inflammation. Based on solubility and pseudo ternary phase diagram tests, ultrafine LORNE composed of Labrafil M 2125 CS, Cremophor RH40, and Transcutol HP to deliver LOR was developed and characterized for its physicochemical properties, emulsification, and *in vitro* release. The selected LORNE was incorporated into carbopol gel (LORNE-Gel) and examined for *ex vivo* skin permeation, retention, dermatokinetics, anti-inflammatory efficacy, and skin irritation. The selected LORNE12-Gel could improve skin permeation, retention, and dermatokinetic results significantly ($p < 0.05$) with enhanced $C_{Skin\ max}$ and $AUC_{0\text{-}48h}$ compared to LOR-Gel. Moreover, LORNE12-Gel showed a remarkable anti-inflammatory effect compared to LOR-Gel after topical application. No signs of skin irritation were observed following treatment, indicating the safety of LORNE12-Gel. Thus, this study demonstrated that LOR-loaded LORNE12-Gel could be promising as an efficient transdermal nanocarrier for an anti-inflammatory alternative.



## 1. Introduction

Lornoxicam (LOR) is a nonsteroidal anti-inflammatory drug with high therapeutic potency of oxicams (Kavitha and Rajendra, 2011). LOR can inhibit the effects of cyclooxygenase enzymes, namely, Type 1 (COX-1) and Type 2 (COX-2) (Radhofer-Welte and Rabassed, 2000). This effect could stop the production of prostaglandin providing systemic analgesic, antipyretic, and anti-inflammatory effects (Helmy et al., 2017). LOR promotes the production of reparative proteoglycans and prevents the release of superoxide radicals and platelet-derived growth factors, both of which are involved in the pathogenesis of inflammation like rheumatoid arthritis (Helmy et al., 2017). In addition, LOR significantly lowers the levels of inflammatory cytokines linked to inflammation mechanisms, such as tumor necrosis factor (TNF), interleukin-1 (IL-1), and nuclear factor Kappa B (NF-κβ) (Isola et al., 2021; Isola et al., 2021). The oral administration of LOR results in inherent side effects after a long period of therapy, such as peptic ulcers and gastric ulcers as the major gastrointestinal side effects. Therefore, this situation is increased due to frequent oral doses of the drug intake, which has been attributed to its lower half-life of 2 to 4 h. LOR doses (8 or 16 mg/day) in chronic inflammation increase the GIT side effects and cardiovascular diseases due to oral repeated doses (Al-Suwayeh et al., 2014). As a result of such complications, LOR has become a suitable candidate for transdermal administration. The advantage of transdermal administration is achieved due to the local incidence of LOR, and the GIT side effects are reduced to a large extent (Londhe et al., 2013).

* Corresponding author at: Department of Pharmaceutics, College of Pharmacy, King Saud University, Building # 23, AA 68, P.O. Box 2457, Riyadh 11451, Saudi Arabia.
*E-mail address:* mbadran@ksu.edu.sa (M.M. Badran).

Peer review under responsibility of King Saud University.

Production and hosting by Elsevier

https://doi.org/10.1016/j.jsps.2023.04.004
1319-0164/

However, classical topical formulations have a low uptake of the drug because of the barrier properties of the stratum corneum (SC). Numerous approaches have been previously adopted to overcome the barrier of SC to enhance the efficacy of skin permeability and increase the driving force of the drug molecule (Badran et al., 2014). In this context, transdermal circulation is primarily evident as the process of direct drug delivery in systematic circulation (Helmy et al., 2017). LOR is a class II drug that shows limited dissolution. Due to the low solubility of LOR, different approaches should be developed to enhance its solubility (Li et al., 2015). Formulation of a drug in lipid-based delivery systems can be used to solve this problem such as liposome, transfersome, emulsion, nanoemulsion, and self-nanoemulsifying drug delivery system (SNEDDS). The SNEDDS formulation can be a more effective carrier for many drugs (Kohli et al., 2010). SNEDDSs are isotropic mixtures that are applied to mix drugs, lipids, and surfactants with cosurfactants (Gursoy et al., 2004). According to BCS, lipid-based delivery systems often involve solubility enhancement of class II drugs where drug bioavailability is governed by drug release properties. SNNEDDSs are good formulations used in *trans*-dermal drug delivery due to their occlusive characteristics on the surface of the skin that hinder the loss of water via the *trans*-epidermal route (Razzaq et al., 2021). SNEDDSs can facilitate the infiltration of the drug through the layers of the skin. Furthermore, the combination of nanosized droplets and topical administration leads to expansion of the surface area of the skin, resulting in better penetration (Ahmad et al., 2020, Razzaq et al., 2021). SNEDDS could significantly increase the time of contact of the encapsulated LOR with SC, leading to more accumulation of the drug (Altamimi et al., 2019). There is a significant lack of research that focuses on the concept of SNEDDSs in the process of transdermal drug delivery systems (Altamimi et al., 2019). A study focused on the analysis of the optimization of the SNEDDS for the enhancement of the *in vivo* hypoglycemic efficacy of glimepiride (GMD) after transdermal use (Ahmed et al., 2014, Razzaq et al., 2021). The research results indicated that GMD-loaded SNEDDSs have significant potential to enhance permeation and associated pharmacokinetic parameters using animal models. Nanoemulsions derived from SNEDSS have been confirmed to not only reduce the SC barrier by dissolving lipids for better drug permeation but also improve drug solubility and reduce skin irritation (Rai et al., 2018). The nanoemulsion is formed by introducing the mixing of oil, surfactant, and a cosurfactant into the aqueous phase coming from the skin layer. SNEDDS could enhance the extent and rate of drug absorption into the systemic circulation due to small droplet size, which allows easier percutaneous transmission, and due to the presence of surfactant and cosurfactant in its composition, which enhances penetration (Xue et al., 2018). The nanoemulsion may improve the hydration of the SC, which improves the drug's skin flux (Badran et al., 2014, Altamimi et al., 2019). Furthermore, an ultrafine SNEDDS formulation (droplet size < 50 nm) is an efficient carrier for transdermal delivery due to its better spreading behavior over the greater surface area of the skin, causing increased drug permeation (Ahmad et al., 2022). Additionally, the enhanced skin permeation of ultrafine SNEDDS is due to the permeation-enhancing ability of its components (Badran et al., 2014). For maximum skin permeation of LOR, the lipid-based nanocarrier hydrogel was formulated for the successful management of inflammation (Hesham et al., 2020). The hydrogel formulation has demonstrated positive prospects in preclinical studies. It has been demonstrated a significant anti-inflammatory effect of the topical application of LOR-loaded nanocarriers (Narahari and Das, 2005). The present study was performed to assess the therapeutic efficacy of the transdermal administration of LOR-loaded SNEDDS gel. However, little work has addressed the effects of LOR-loaded nano-systems when administered transdermally. Therefore, the study aimed to develop LOR-loaded SNEDDS-Gel to target skin layers by improving its permeation. LOR-loaded SNEDDSs were prepared and characterized for solubility, size, entrapment, and *in vitro* release. The LOR-loaded SNEDDS was further loaded into the gel and characterized for *ex vivo* skin retention, dermatokinetic study, anti-inflammatory activity, and skin irritation.

## 2. Experimental

### 2.1. Materials

Lornoxicam (LOR) was kindly provided by Al Jazeerah Manufacturing Co. Riyadh KSA. Larbafil M 2125 CS, Labrafac, Labrasol (caprylcaproyl macrogol glycerides), Transcutol HP (diethylene glycol monoethyl ether), Peceol (glyceryl monooleate) and Capmul®MCM were purchased from Gattefosse (Saint-Priest Cedex, France). Cremohpor® RH 40, Cremophor® EL, and Cremophor® ELP were purchased from BASF (Ludwigshafen, Germany). Oleic acid and ethyl oleate were procured from Acros Organics, USA. Isopropyl myristate (IPM), glycerol, Tween80, Tween20, PEG 400 (polyethylene glycol 400), 1,2-propylene glycol, methanol, and sodium acetate were purchased from BDH Laboratory Supplies (BDH Chemicals Ltd., Poole, England). High-purity water was obtained through a Milli-Q Integral Water Purification System (Millipore, Bedford, MA, USA). All other chemicals used were of analytical reagent grade.

### 2.2. HPLC analysis of LOR

Reverse HPLC was used to measure the content of LOR with minor modifications (Taha et al., 2018). A Waters Model 1515 HPLC pump, Waters Autosampler Model 717 plus, and Waters 2487 dual absorbance UV detector made up the HPLC system, which was controlled by a computer running Empower software (version 1154). This procedure used 0.1 M sodium acetate solution and methanol as the mobile phase (50:50). The mobile phase was freshly produced, filtered through a 0.45 m Millipore filter under vacuum, and degassed before use. The mobile phase (1 mL/min) was supplied via a C18 analytical, Hypersil™ MOS column (150 mm in length, 4. 6 mm in diameter, and 5 m particle size) at a temperature of 35 °C. LOR was quantified using isocratic elution. The injection volume was 20 μL, and UV detection was performed at a wavelength of 278 nm.

### 2.3. Screening of oils, surfactants, and cosurfactants

The solubility of LOR in several oils, surfactants, and cosurfactants was investigated. An excess amount of LOR was added to a clean glass vial containing 1 g of each component and vortexed for 30 sec. Following proper sealing, the vials were mechanically shaken in a water bath shaker at 37 °C for 72 h to reach equilibrium (Li et al., 2015). Each sample was centrifuged at 10000 rpm for 20 min. The supernatant fraction was then collected and dissolved in methanol. The amount of soluble LOR was determined using HPLC after proper dilution with the mobile phase. The experiment was performed in triplicate, and the solubility was then recorded as mg/g.

### 2.4. Pseudoternary phase diagram

Labrafil M 2125 CS, Cremophor RH40, and Transcutol HP were selected as oil phase surfactants and cosurfactants, respectively, due to their high solubility of LOR. Deionized water was employed as the aqueous phase. An aqueous titration technique was used to build the pseudoternary phase diagrams (Shakeel et al., 2014).

Three mixtures of surfactant and cosurfactant ($S_{mix}$) were prepared in ratios of 1:1, 2:1, and 3:1. Each mixture was mixed with the oil phase in a ratio ranging from 1:9 to 9:1. Each combination was titrated slowly with deionized water under vortexing at 25 °C. The obtained mixtures were then checked visually for the formation of a clear or transparent emulsion. The ratios of oil, $S_{mix}$, and distilled water that formed clear emulsions were used for the pseudoternary phase diagram (Zafar et al., 2021). Based on the phase diagrams, the amount of each component was selected for the preparation of LOR-loaded SNEDDS (LORNE).

### 2.5. Preparation and characterization of LORNE

#### 2.5.1. Determination of LOR solubility in LORNE

To produce stable LORNE with maximum loading in various SNEDDS formulations, LOR solubility in LORNE is needed. Thus, various LORNE formulations from the nanoemulsion area of phase diagrams were prepared. Briefly, an excess amount of LOR (5 mg/g) was added to a vial during the preparation of 1 g of each SNEDDS formulation. After sealing the vials, vortexing was used to help solubilizing LOR. Then, they were shaken at 25 °C for 72 h in a shaking water bath, followed by equilibrium for 24 h to examine any sign of phase separation. The undissolved LOR was then removed from the SNEDDS using centrifugation at 10000 rpm for 20 min at 37 °C. After separation, the supernatant was dissolved in methanol and then diluted in a mobile phase solution. The experiments were conducted three times, and the solubility (mg/g) of LOR was measured by HPLC. Afterward, SNEDDS formulations with maximum LOR solubility were used for the following experiments.

#### 2.5.2. Self-emulsification time

Following the emulsification process, visual observation was used to determine the self-emulsification time for each LORNE (Beg et al., 2012). Using a stopwatch, the required time in seconds to obtain a clear dispersion was determined after proper dilution with double distilled water at 1:50. The emulsion's appearance was observed and classified as transparent, translucent, and cloudy.

#### 2.5.3. Droplet size distribution and zeta potential measurements

The droplet size of the selected LOR-SNEDDS was determined using dynamic light scattering by a Zetasizer Nano ZS (Malvern Instruments Ltd., Worcestershire, UK). LORNE was homogeneously dispersed in double distilled water at 1:50 and mixed for 1 min using vortexing to assure homogeneity. The droplet size (z-ave) and polydispersity index (PDI) were determined. Additionally, the zeta potential was measured with the help of a Zetasizer Nano ZS based on the electrophoretic mobility. Data are expressed as the mean ± standard deviation (SD) of three replicates.

#### 2.5.4. In vitro drug release

An *in vitro* release study was carried out using vertical Franz diffusion cells for the selected LORNE based on the visual assessment, droplet size, and emulsification time. The cellulose membrane (molecular weight cutoff 14,000) was used after soaking in phosphate buffer (PBS, pH = 7.4) overnight. This membrane was mounted onto the Franz diffusion cell with a diffusional area of 1.76 cm2. The receptor phase contained 12 mL of PBS and was maintained at 37 °C with constant stirring. In the donor compartment of the Franz cell, an equivalent volume of LOR SNEDDS containing 0.5 mg LOR was introduced. A precise sample (1 mL) was taken at intervals of 0.5, 1, 1.5, 2, 4, 6, 8, 24, and 48 h. To maintain a constant volume, an equal volume of the dissolution medium was added to maintain sinking conditions during the whole experiment. LOR released from SNEDDS formulations was measured using HPLC and compared to LOR suspension in PBS (1 mg/mL). All measurements were performed in triplicate.

#### 2.5.5. Transmission electron microscopy (TEM)

The LORNE formulations were visualized by TEM of the selected formulations based on the droplet size, emulsification time, and drug release results. The morphology of LORNE was observed by TEM (JEOL Co., JEM-2100, Tokyo, Japan) under an accelerated voltage of 80 kV. LORNE was diluted with double distilled water (1:50). A sample drop was placed on a carbon-coated copper grid and air-dried for 10 min. The excess was immediately removed using filter paper and then negatively stained with 2% (w/v) uranyl acetate solution for 1 min. At the proper magnifications, the shape and surface features were then assessed.

### 2.6. Hydrogel preparation of LORNE and LOR

The highest-release LORNE formulations were selected for further experiments. Therefore, LORNE10, LORNE11, and LORNE12 were added to 1% w/w carbopol 934 hydrogels. Briefly, carbopol 934 was weighed out and dispersed in distilled water, followed by stirring at room temperature for 3 h. Triethanolamine (0.5% w/v) was applied to raise the pH to 7. The cross-linking between triethanolamine and carbopol 934 was promoted by preserving the gel bases overnight. At room temperature, the gel base was mixed with an equal amount of the selected LORNE under stirring to obtain a homogenous clear mixture to obtain LORNE10-Gel, LORNE11-Gel, and LORNE12-Gel.

#### 2.6.1. Evaluation of LORNE and LOR gels

Drug content was estimated by weighing 1 g of each gel followed by dissolving in methanol in a 100 mL volumetric flask and stirring to dissolve the gel completely at 37 °C for 24 h. After that, the solution was properly diluted with the mobile phase and filtered (0.45 μm membrane) to determine LOR content by HPLC.

The pH of LORNE Gels was determined using a Mettler Toledo Seven Compact pH meter (Billerica, MA) maintained at 37 °C. Before every run, the pH meter was calibrated using typical buffer solutions with pH values of 4, 7, and 10. Each sample reading was obtained in triplicate after a pH electrode was dipped directly into the gel.

The viscosity of the formulations (0.5 g) was determined without dilution using a Brookfield DV III ultra V6.0 RV cone and plate rheometer (Brookfield Engineering Laboratories, USA) using spindle #CPE40 at 25 ± 3 °C.

#### 2.6.2. Ex vivo skin permeation studies of LORNE and LOR gels

Ex vivo skin permeation tests were conducted on abdominal rat skin. The abdominal hair was shaved using a hair clipper. By using a scalpel and surgical scissors, the skin was removed from each rat, and the subcutaneous fat and connective tissues were separated. The removed skin samples were then examined for integrity after being rinsed with normal saline. The skin samples were then kept at a temperature of −20 °C in aluminum foil until they were used within two weeks. All studies were carried out according to the Guidelines of Research Ethics Committee of King Saud University College of Pharmacy, Riyadh, Saudi Arabia (Ref. No.: KSU-SE-18–23).

*The in vivo* efficacy of a transdermal formulation is always influenced by the amount of penetrant and extent of permeability of the skin. Therefore, *ex vivo* permeability studies of LORNE10-Gel, LORNE11-Gel, and LORNE12-Gel were conducted in comparison to LOR-Gel. The prepared skin samples were mounted onto Franz diffusion cells (Logan Instrument Corp., NJ, USA) with a diffuse area of 1.7 $cm^2$ and a receptor volume of approximately 12 mL PBS (pH

7.4) with 0.01% w/v sodium azide. To simulate the *in vivo* situation, the receptor fluid was maintained at 37 °C (i.e., 32 °C for skin) and 500 rpm of magnetic stirring. A certain amount of LORNE-Gels (0.5 mg of LOR) was spread on the donor compartment. All experiments were performed with the occluded condition. The sample aliquots were taken out of the receptor at 0.5, 1, 1.5, 3, 6, 8, 12, 24, 30, and 48 h and replaced by an equal volume of fresh PBS pH 7.4 solution to maintain sinking conditions.

The steady state of LOR flux ($J_{ss}$, μg/cm$^2$.h) and permeability coefficients (Kp, cm$^2$/h) were calculated from the results of *ex vivo* skin permeation. The lag time ($T_L$) was also determined. To determine the degree of enhancement, an enhancement ratio (ER) was calculated by dividing the $J_{ss}$ of the respective LORNE-Gel by the $J_{ss}$ of the control LOR-Gel.

*2.6.3. Ex vivo skin retention and dermatokinetic studies of LORNE and LOR gels*

The skin samples were properly cleaned off by PBS to eliminate the remaining formulations after the completion of *ex vivo* skin permeation studies. The skin samples were attached to cork plates and stretched using small pins. The SC was collected by tape-stripping using 3 M Transpore™ tape (St. Paul, MN, USA). Ten tap strips were cut into 2 × 2 cm$^2$ pieces, pressed onto the treated skin area, and removed successively after pressure on a defined area of SC immediately. The initial tape strip was thrown away because of the risk of contamination from any LOR that could have remained on the skin's surface. After stripping, the remaining skin samples were sliced into small pieces. For complete LOR extraction, the SC tapes and pieces of stripped skin were immersed individually in 80% of the methanolic PBS solution overnight, followed by 5 min of vortexing and 5 min of sonication. HPLC was used to determine the LOR content in the SC, stripped skin, and receptor fluid after proper filtering. With more than 90% of the recovered LOR, the extraction effectiveness of 80% methanolic PBS (pH 7.3) was validated. Each experiment was run in triplicate. The skin retention study was carried out according to the Guidelines of Research Ethics Committee of King Saud University College of Pharmacy, Riyadh, Saudi Arabia (Ref. No.: KSU-SE-18–23). The desired formulation was selected for the dermatocokinetic investigation at different times in SC and stripped skin layers. The same retention study procedure was conducted to determine the dermatokinetics. Dermatokinetics were estimated for LOR retention in different skin layers and its elimination after 1, 3, 6, 12, and 24 h of sample application. The skin samples were properly cleaned off to eliminate the unabsorbed drug, attached to cork plates and stretched using small pins. The stripping technique was used to separate SC, and the remaining skin samples were chopped into small pieces. HPLC was used to determine the LOR concentration in SC and the stripped skin samples. The concentration of LOR (μg/cm$^2$) assessed in skin layers (SC and stripped skin) was plotted, and dermatokinetic parameters were evaluated. The noncompartmental pharmacokinetic model was used for the calculation of $T_{max}$, $C_{Skin\text{-}max}$, $AUC_{0\text{-}48h}$, and Ke (Rapalli et al., 2021). Each experiment was run in triplicate.

*2.6.4. Anti-inflammatory studies of LORNE and LOR gels*

A rat paw edema test caused by carrageenan was used as a model for *in vivo* acute anti-inflammatory activity (Wada et al., 1982). The anti-inflammatory activity was carried out according to the Guidelines of Research Ethics Committee of King Saud University College of Pharmacy, Riyadh, Saudi Arabia (Ref. No.: KSU-SE-18–23). Six groups of 200–250 g rats were used (6 animals each). The first group received the plain gel, the second group received phenylbutazone (PBZ), and the third and fourth groups were treated with LOR-Gel and LORNE12-Gel, respectively. PBZ was given as a reference group. The right hind paw surface was treated with the formulations, and the treated area was immediately covered with gauze and a thin vinyl sheet. The covers were removed after 2 h, and 0.1 mL of 1% carrageenan solution was subcutaneously injected into the treated area as well as the left hind paw. By using a digital plethysmometer, the volume of paw edema (measured in mL) in each animal was determined. Before injecting carrageenan, the initial paw volume of the rats was assessed by dipping the paw into the electrolyte column, and the subsequent rise in volume due to fluid displacement was recorded from a digital monitor (El-Megrab et al., 2006). After 1, 2, 3, 6, and 8 h of topical application, the paw volume was measured. The % inhibition of edema was utilized as an indicator of anti-inflammatory activity. The swelling of the treated animal was compared to the swelling of a control group. The following equation was used to determine the inhibition of paw edema:

% Paw edema inhibition = (Swelling of control group-% Swelling of treated group)/(% Swelling of control group) × 100.

*2.6.5. Skin irritation study of selected LORNE and LOR gels*

Male albino Wistar rats (200–250 g) were kept in cages with free access to water and a regular laboratory diet. The hairs on the rat dorsal were shaved a day before the experiment. The rats were divided into group I, which served as a negative control, and group II, which was used as a positive control (using 0.8% v/v formalin as a standard irritant) (Elmowafy et al., 2019). LOR-Gel (0.5 g) was applied to group III, while LORNE12-Gel (0.5 g) was applied to group IV. After 8 h of application, the formulation was removed, and skin erythema was visually noted as a sign of irritation. The Draize scale was used as an indicator of irritation as follows: 0 points: no erythema, 1 point: very slight erythema, 2 points: well-defined erythema, 3 points: moderate to severe erythema, and 4 points: severe erythema (Elmowafy et al., 2019).

*2.7. Statistical data analysis*

Data analysis was carried out with the software package Microsoft Excel, Version 2010, and Origin software, version 8. The results are expressed as the mean ± standard error (n = 3). When comparing three or more conditions, one-way analysis of variance (ANOVA) was performed.

## 3. Results

*3.1. Solubility studies*

In this study, the solubility of LOR was examined using several excipients to produce a successful SNEDDS formulation. Therefore, the solubility of LOR in different oils, surfactants, and cosurfactants is displayed in Fig. 1. LOR showed the highest solubility in Labrifil M 2125 CS (0.892 ± 0.037 mg/g), followed by oleic acid (0.685 ± 0.02 3 mg/g), IPM (0.375 ± 0.022 mg/g), and ethyl oleate (0.089 ± 0.01 5 mg/g) as an oily phase. In addition, Cremophor RH40 exhibited the maximum solubility of LOR (6.921 ± 0.044 mg/g) as an investigated surfactant (Fig. 1B). Cremophor EL (4.622 ± 0.081 mg/g) and Cremophor ELP (1.055 ± 0.062 mg/g) showed lower solubility of LOR than Cremophor RH40. Moreover, the solubility of LOR in Tween 80 and Tween 20 was 5.752 ± 0.059 mg/g and 3.392 ± 0.44 2 mg/g, respectively. Meanwhile, the solubility of LOR in cosurfactants was 1.631 ± 0.034 mg/g, 1.582 ± 0.028 mg/g, and 0. 234 ± 0.012 in Transcutol HP, PEG400, and glycerol, respectively (Fig. 1C).

Consequently, the selected oil, surfactant, and cosurfactant phases were Labrafil M 2125-CS, Cremophor RH 40, and Transcutol HP, respectively.

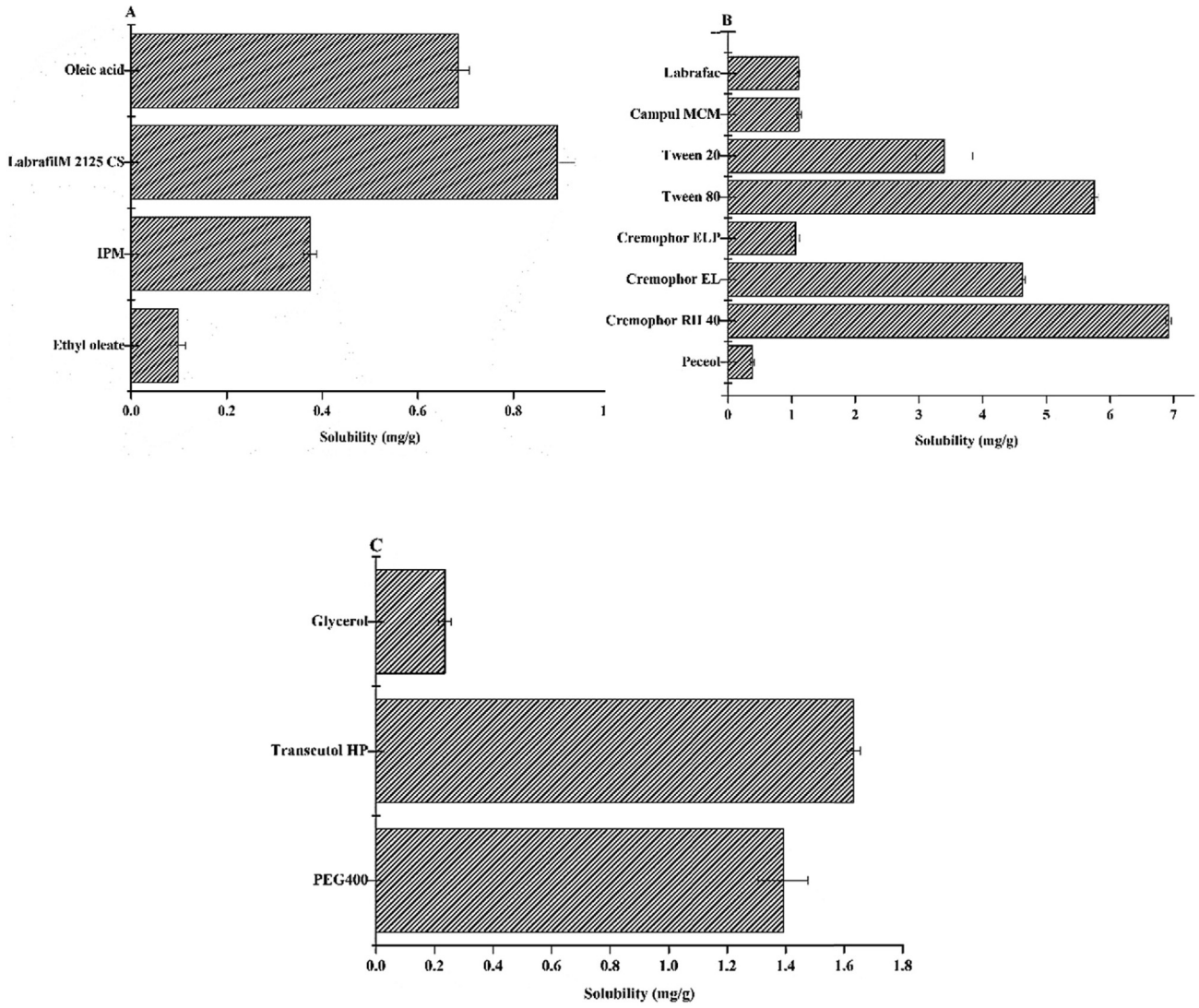


**Fig. 1.** Solubility of LOR (mg/g) in various oils (A), surfactants (B), and cosurfactants (C) at 37 °C. Data are expressed as the mean ± SD, n = 3.

### 3.2. Pseudoternary phase diagram

The pseudoternary phase is essential in designing the obtained area of nanoemulsions and determining the proper percentage of components needed for SNEDDS formulations. It formed from Cremophor RH 40 and Transcutol HP as $S_{mix}$ in several ratios of 1:1, 2:1, and 3:1 with Labrafil M 2125 CS as oil (Fig. 2). Accordingly, the Smix ratio of 3:1 produced the largest nanoemulsion area for the SNEDDS. Furthermore, $S_{mix}$ ratios of 2:1 and 1:1 exhibited a decrease in the nanoemulsion area. After identification of the self-emulsifying region, the desired excipient ratios of SNEDDS were pooled randomly for LOR incorporation (LORNE) (Table 1). After water dilution, stable nanoemulsions may be produced by gentle agitation using these components of oil/$S_{mix}$ ratios, and LORNE formulations could then be employed for further investigations.

### 3.3. Characterization of the selected LORNE

#### 3.3.1. Determination of LOR solubility in LORNE

A fixed LOR concentration was selected to be loaded into all LORNE using a lower concentration than the minimal saturation solubility (Table 2). The fixed concentration of LOR could offer spontaneous emulsification of LORNE after aqueous dilution with a minor possibility of drug precipitation (Narag et al., 2007). Then, the LOR solubility in LORNE formulations was employed and further characterized for the selection of the desired formulation. For a more direct comparison among the LORNE formulations, 1 mg of LOR was loaded in 1 g of each SNEDDS formulation. The desired SNEDDS could offer a chance to improve LOR's *in vitro* and *in vivo* performance, thereby making it a perfect delivery carrier.

#### 3.3.2. Evaluation of emulsification time

The emulsification time was less than 30 (Table 2), which proved their capacity to disperse completely and quickly when exposed to aqueous dilution under gentle stirring. The short self-emulsification time of the most obtained LONE was correlated with the increased concentration of surfactant. The clear nanoemulsions were indicated by the clarity and transparency of the formed nanoemulsions. Otherwise, bad formulations showed a coarse emulsion with a cloudy appearance and bulky size.

#### 3.3.3. Droplet size distribution and zeta potential measurements

The droplet size is usually influenced by the type and concentration of surfactants and oil used in the formulation. The obtained

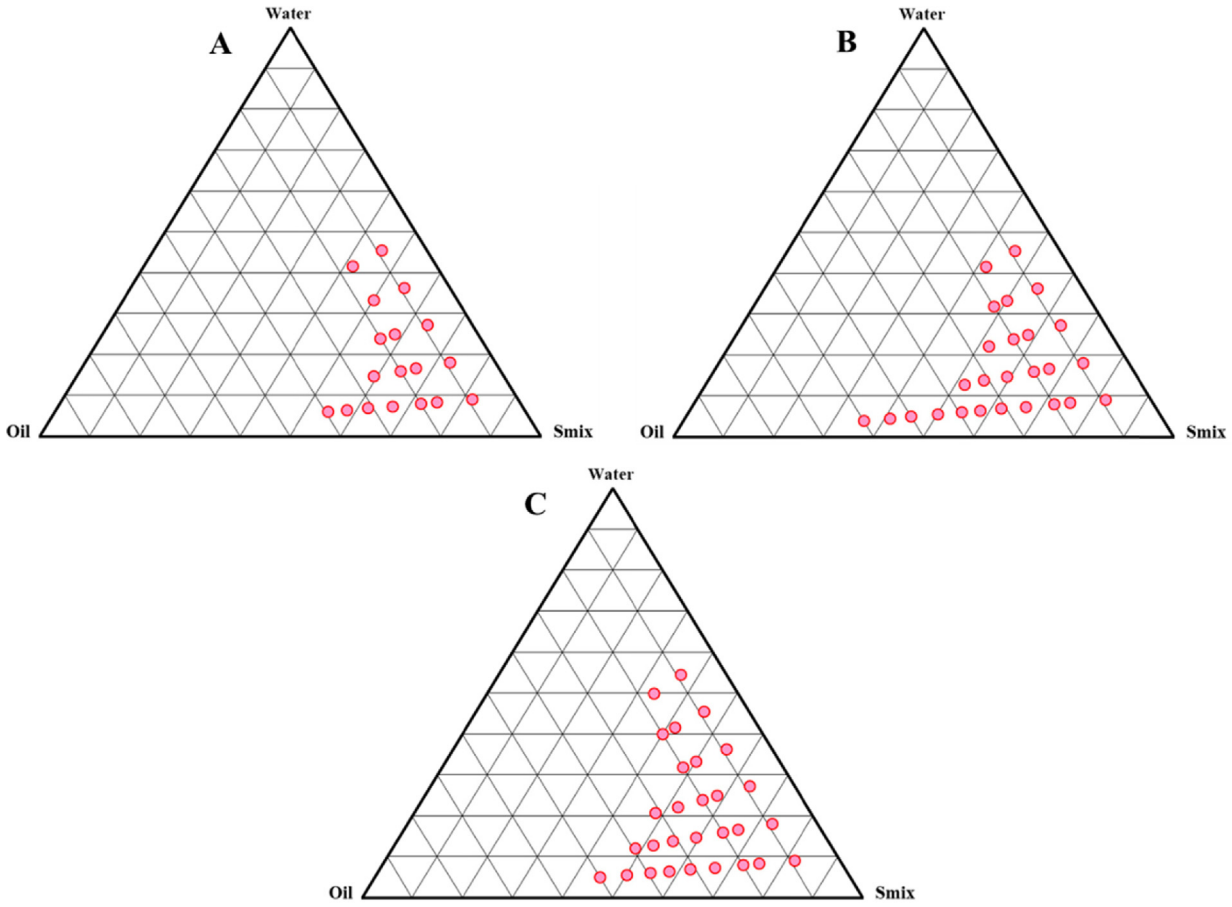


**Fig. 2.** Pseudoternary phase diagrams of Labrafil M 2115 CS, Cremophor RH40, and Transcutol HP indicating the o/w nanoemulsion region at $S_{mix}$ (1:1) (A), $S_{mix}$ (2:1) (B) and $S_{mix}$ (3:1) (C).

**Table 1**
Formulation components (%, w/w) of LORNE prepared using Labrafil M2125 CS (oil phase), Cremophor RH40 (surfactant), Transcutol-HP (cosurfactant), and deionized water (aqueous phase).

| Formulation Codes | Labrafil M2125CS | $S_{mix}$ | Cremophor RH40 | TranscutolHP | Water |
|---|---|---|---|---|---|
| | Oil | | Surfactant | Cosurfactant | Oil |
| LORNE1 | 10 | 1:1 | 25 | 25 | 40 |
| LORNE2 | 15 | 1:1 | 30 | 30 | 25 |
| LORNE3 | 20 | 1:1 | 30 | 30 | 20 |
| LORNE4 | 10 | 2:1 | 40 | 20 | 30 |
| LORNE5 | 15 | 2:1 | 44 | 21 | 20 |
| LORNE6 | 20 | 2:1 | 47 | 23 | 10 |
| LORNE7 | 15 | 2:1 | 50 | 25 | 10 |
| LORNE8 | 10 | 3:1 | 30 | 10 | 50 |
| LORNE9 | 10 | 3:1 | 38 | 12 | 40 |
| LORNE10 | 15 | 3:1 | 45 | 15 | 25 |
| LORNE11 | 20 | 3:1 | 49 | 16 | 15 |
| LORNE12 | 20 | 3:1 | 53 | 17 | 10 |

results revealed that the droplets of certain nanoemulsions are in the ultrafine nanometric range (<50 nm), as the average droplet size of the LORNE ranged from 38 to 172 nm (Table 3). As the surfactant concentration in the $S_{mix}$ increased, the LORNE droplet size decreased. The PDI displays the size distribution of the nanoemulsion and reflects the uniformity of the droplet diameter. A PDI value of 0.1–0.25 indicates a narrow size distribution, while a PDI > 0.5 indicates a broad distribution. PDI was less than 0.5, which indicates a uniform droplet size distribution (Shafiq et al., 2007). Zeta potential is also a highly significant factor in characterizing emulsification efficacy (Ahmad et al., 2022). The impact of the zeta potential depends on its value, which confirms the stabilization of nanocarriers. The zeta potential value indicates the magnitude of the repulsion between the similarly charged particles in the dispersion (Ahmad et al., 2020). The results proved the negative charge of the SNEDDS formulations, with values ranging from −8 to −23 mV, indicating a stable system with well-separated globules.

### 3.3.4. *In vitro* LOR release study

Four LORNE were selected for the *in vitro* release experiment based on the findings of particle size analysis, solubility and

**Table 2**
Solubility and evaluation of various LORNE formulations.

| Formulation Codes | Solubility (mg/g) | Appearance | Emulsification time (sec) | Visual assessment |
|---|---|---|---|---|
| LORNE1 | 1.959 ± 0.373 | Cloudy | 23 | Bad |
| LORNE2 | 2.248 ± 0.164 | Cloudy | 22 | Bad |
| LORNE3 | 2.334 ± 0.186 | Cloudy | 23 | Bad |
| LORNE4 | 2.585 ± 0.217 | Transparent | 21 | Good |
| LORNE5 | 2.736 ± 0.673 | Transparent | 22 | Good |
| LORNE6 | 2.833 ± 0.091 | Transparent | 23 | Good |
| LORNE7 | 3.249 ± 0.481 | Transparent | 17 | Good |
| LORNE8 | 3.193 ± 0.264 | Transparent | 19 | Good |
| LORNE9 | 2.902 ± 0.151 | Transparent | 17 | Good |
| LORNE10 | 3.453 ± 0.248 | Transparent | 15 | Good |
| LORNE11 | 3.741 ± 0.174 | Transparent | 16 | Good |
| LORNE12 | 3.934 ± 0.126 | Transparent | 17 | Good |

**Table 3**
Droplet size, DPI, and ζ-potential of LORNE formulations.

| Formulation Codes | Droplet size (nm) | PDI | ζ - Potential (mV) |
|---|---|---|---|
| LORNE1 | 137.9 ± 7.4 | 0.45 ± 0.05 | − 8.2 ± 0.6 |
| LORNE2 | 148.2 ± 4.6 | 0.41 ± 0.04 | − 10.3 ± 0.9 |
| LORNE3 | 171.6 ± 6.3 | 0.48 ± 0.05 | − 9.1 ± 0.3 |
| LORNE4 | 115.0 ± 3.9 | 0.32 ± 0.04 | −10.4 ± 0.6 |
| LORNE5 | 102.7 ± 3.8 | 0.08 ± 0.02 | − 12.5 ± 1.8 |
| LORNE6 | 58.1 ± 3.6 | 0.24 ± 0.07 | − 16.2 ± 1.9 |
| LORNE7 | 53.0 ± 2.8 | 0.22 ± 0.06 | − 18.3 ± 2.5 |
| LORNE8 | 81.1 ± 4.7 | 0.17 ± 0.01 | −13.5 ± 1.4 |
| LORNE9 | 92.5 ± 4.5 | 0.09 ± 0.00 | − 11.3 ± 1.7 |
| LORNE10 | 47.4 ± 3.6 | 0.11 ± 0.01 | − 17.2 ± 1.3 |
| LORNE11 | 41.3 ± 5.1 | 0.07 ± 0.00 | − 18.0 ± 1.3 |
| LORNE12 | 37.6 ± 4.2 | 0.16 ± 0.213 | −23.1 ± 3.2 |

emulsification time. In comparison to the LOR suspension (LOR control), the drug release from LORNE was considerably higher. The lowest release rates were detected in LORNE9 compared to LORNE10, LORNE11, and LORNE12 (Fig. 3). The increased solubilization of LOR in Cremophor RH 40 and Transcutol HP may explain the high drug release values in LORNE (higher availability of LOR). Additionally, when the droplet size decreases, a greater interfacial surface area is provided (Heshmati et al., 2013), leading to more released drugs. Greater drug release (85.7%) was observed with LORNE12 after 48 h compared to 77.2%, 68.4%, and 49.3% of LORNE11, LORNE10, and LORNE9, respectively. The lowest amount of released LOR (9.2%) from the control was observed. Here, the drug release profiles were statistically significant ($p < 0.05$).

### 3.3.5. Transmission electron microscopy (TEM)

TEM was used to visualize the morphology of LORNE10, LORNE11, and LORNE12 due to their high drug release. The TEM images are represented in Fig. 4. The images showed the spherical shape of the nanoemulsions, with no signs of coalescence. The droplet size was found to be in agreement with that determined by DLS. The observed droplets seemed uniform and nonaggregated with no signs of precipitation, which indicated the physical stability of the obtained nanoemulsion.

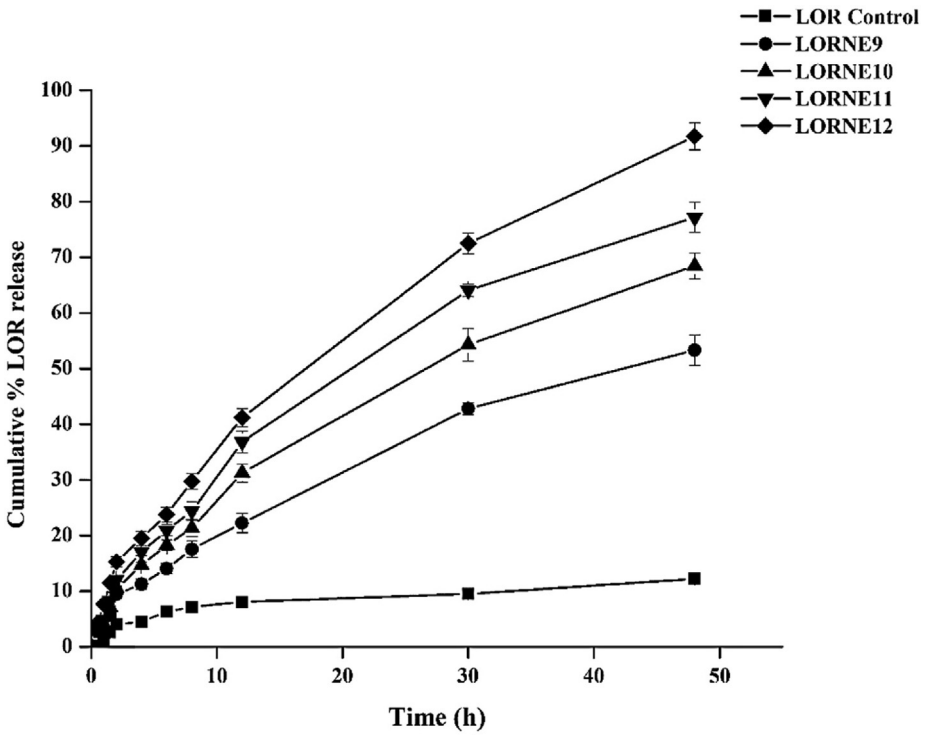


**Fig. 3.** *In vitro* release profiles of the selected SNEDDS (LORNE) and LOR control (n = 3, mean ± SD).

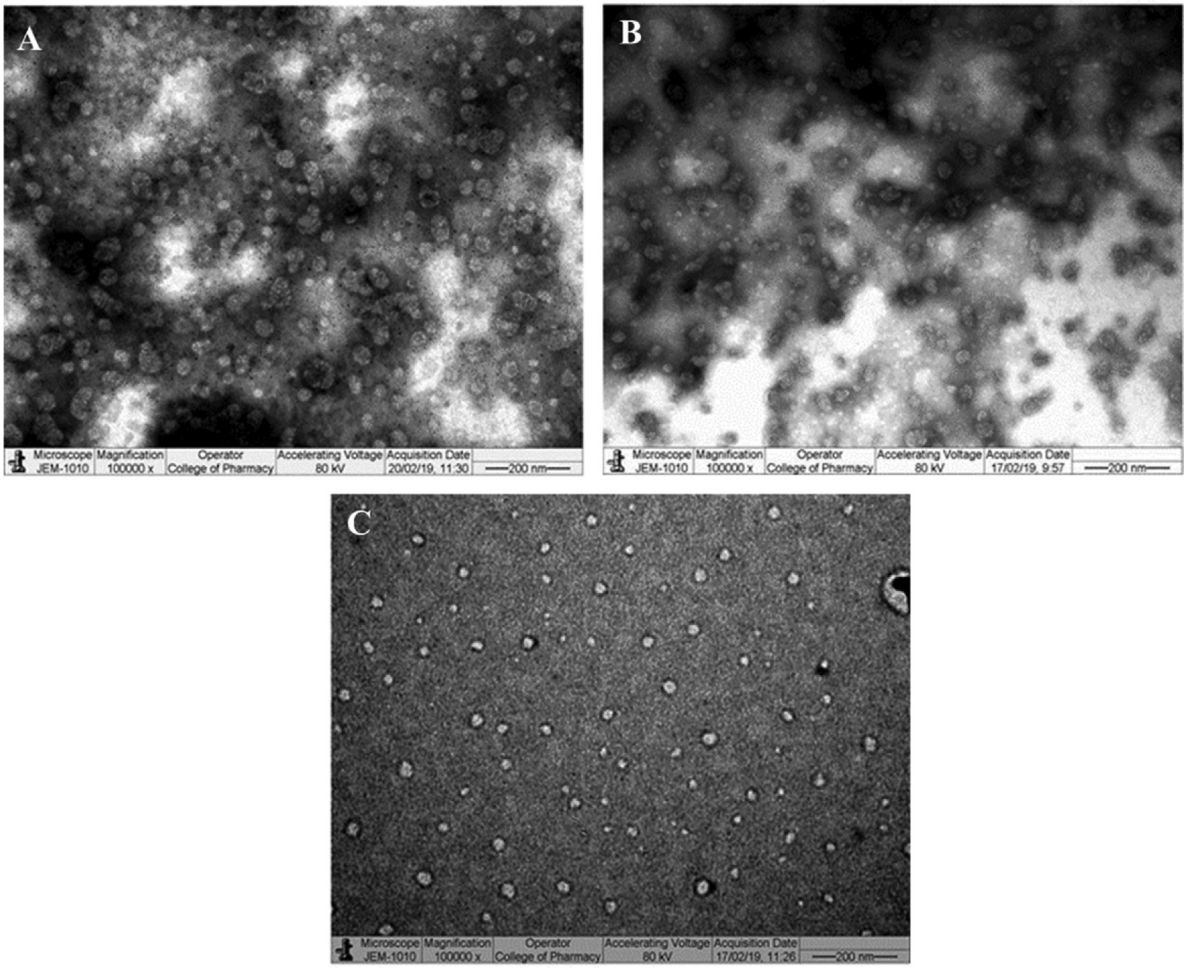


**Fig. 4.** TEM images of LORNE10 (A), LORNE11 (B), and LORNE12 (C).

### 3.4. Hydrogel preparation of LORNE and LOR

The formulations LORNE 10, LORNE 11, and LORNE 12 were selected for skin permeation and retention based on the highest drug release. To extend the contact time between the LOR and the skin surface, the carbopol was used to retain the skin surface. Therefore, carbopol 934 was selected as a gel-forming polymer due to its adhesive features, swelling propensity, biocompatibility, and hydrophilic nature of o/w nanoemulsions. The hydrogel polymeric network of carbopol permits high water absorption. When the polymer level is close to 1%, nanoemulsion hydrogels are appropriate for topical and transdermal distribution (Lapasin et al., 2001).

#### 3.4.1. Evaluation of LORNE and LOR gels

The pH of the obtained formulations ranged from 5.7 to 5.8, which is within the pH range of skin causing less irritation (Chen et al., 2016). The average LOR content of the gel formulations was 91 and 96%. According to the Pharmacopoeia, the drug content uniformity of topical semisolid preparations should be in the range of 90 to 110% (Ueda et al., 2009). The LOR contents of LORNE10-Gel, LORNE11-Gel, and LORNE12-Gel were 91.21%±1.46, 96.47%±1.68 and 96.26%±1.98, respectively, indicating acceptable content uniformity. The low viscosity of the SNEDDS formulations makes it challenging for skin application. Therefore, a viscous formulation using carbopol 934 gel was used to overcome this drawback, making it perfectly adapted for topical claims (Zheng et al., 2016). SNEDDS-loaded Carbopol 934 gels may prolong skin contact, increasing the permeated amount of LOR through the skin (Lala et al., 2014). The viscosity was changed by increasing the shear rate. The gel systems of LORNE11-Gel and LORNE12-Gel have a higher viscosity than LORNE10-Gel and LOR control. This may be because LORNE11-Gel and LORNE12-Gel contain more oil than LORNE10-Gel. The values of their viscosity can be ordered as follows: LORNE10-Gel > LORNE11-Gel > LORNE12-Gel and LORNE-Gel.

#### 3.4.2. Ex vivo skin permeation studies of LORNE and LOR gels

*Ex vivo* skin permeation experiments were conducted for 48 h (Fig. 5). There was a significant difference in the permeated amount of LOR through the skin between LORNE10-Gel, LORNE11-Gel, and LORNE12-Gel compared to LORNE-Gel ($P < 0.05$). Compared to LORNE10-Gel and LORNE11-Gel, LORNE12-Gel had the maximum permeated amount of LOR over 48 h. The results showed that LOR-Gel had the lowest *ex vivo* permeation rate, with just 59.43 ± 8.93 μg/cm$^2$ of the loaded LOR permeated after 48 h. However, the permeated amount of LOR from LORNE12-Gel was greatly improved to 356.29 ± 17.18 μg/cm$^2$ at 48 h. *Ex vivo* LOR permeation rates from LORNE11-Gel and LORNE10-Gel were 241.21 ± 12.26 μg/cm$^2$ and 151.28 ± 14.45 μg/cm$^2$, respectively, at 48 h.

Table 4 represents the data of the steady-state flux (*Jss*), permeability coefficient (Kp), and lag time. The permeation process is not governed by the gradient of drug concentration because all

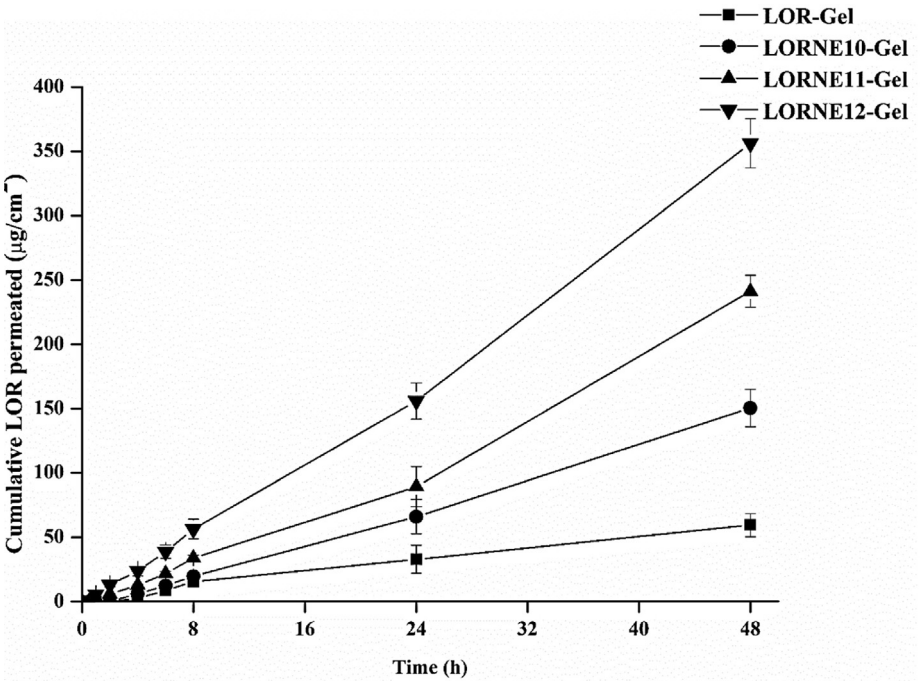


**Fig. 5.** Comparative *ex vivo* permeation profiles of LORNE10-Gel, LORNE11-Gel, LORNE12-Gel, and LOR-Gel formulations through the rat skin membrane as a skin model.

**Table 4**
LOR transdermal permeation parameters of LOR-Gel, LORNE10-Gel, LORNE11-Gel, and LORNE12-Gel formulations through the rat skin membrane as a skin model.

| Formula codes | Flux, $J_{ss}$ ($\mu g/cm^2/h$) | Permeability coefficient $Kp*10^{-3}$($cm\ h^{-1}$) | Lag time (h) | Enhancement ratio (ER) |
|---|---|---|---|---|
| LOR-Gel | 1.255 ± 0.754 | 1.492 ± 0.737 | 4.405 ± 0.976 | – |
| LORNE10-Gel | 3.274 ± 0.427 | 4.354 ± 0.761 | 2.491 ± 0.266 | 2.662 |
| LORNE11-Gel | 5.229 ± 0.646 | 6.385 ± 0.685 | 2.153 ± 0.699 | 4.960 |
| LORNE12-Gel | 8.181 ± 0.611 | 9.269 ± 0.854 | 1.481 ± 0.763 | 6.5 |

SNEDDS-gel and control formulations have an equal LOR load. LORNE12-Gel has a maximum transdermal *Jss* value of 8.2 μg/$cm^2$/h, which is almost 6.3 times greater than the value of LOR-Gel (1.3 g/$cm^2$/h). The transdermal *Jss* for LORNE11-Gel was 5.3 μg/$cm^2$/h, while LORNE10-Gel showed a transdermal *Jss* of 3.2 μg/$cm^2$/h, which was consistent with their reduced solubility result. Compared to LOR-Gel, all LORNE-based gels showed considerably greater Kp following occlusion application ($P < 0.05$). In addition, Kp was significantly greater in LORNE12-Gel than in other LORNE-based gels. *Kp* was determined to be $9.2 \times 10^{-3}$, $6.4 \times 10^{-3}$, and $4.4 \times 10^{-3}$ for LORNE12-Gel, LORNE11-Gel, and LORNE10-Gel, respectively (Table 4). There was a significant variation in the lag time for SNEDDS-gel formulations. The lag times for LORNE12-Gel, LORNE11-Gel, LORNE10-Gel, and LOR-Gel were 1.5, 2.2, 2.5, and 4.4, respectively (Table 4). LORNE12 showed the highest transdermal Jss and Kp values due to its comparatively high $S_{mix}$ concentration, small droplet size, and high solubility. LORNE10 has less $S_{mix}$, which could be the reason for the decreased value of Jss and KP (Zhao et al., 2006). Drug control has a long lag time since LOR incorporated into gel bases takes a long time to release from the polymer (Rizwan et al., 2010). As a result, LORNE's lag time was reduced, supporting the efficacy of surfactants and cosurfactants as permeation enhancers. ER was found to be highest in the LORNE12-Gel formulation compared with the other formulations.

### *3.4.3. Ex vivo skin retention and dermatokinetics studies of LORNE and LOR gels*

The ability of SNEDDS to deliver LOR into different skin layers was investigated using rat skin. Fig. 6 represents the skin retention of LOR delivered from LOR-Gel, LORNE10-Gel, LORNE11-Gel, and LORNE12-Gel. The retention of LOR in different skin layers was significantly improved by using LORNE. LORNE12 showed the highest retained amount of LOR in different skin layers compared to other formulations ($p < 0.05$). A significant increase in the amount of LOR with LORNE12 in SC and stripped skin was 3.7-fold and 7.1-fold, respectively, compared to LOR-Gel. LORNE11 showed a 2.6-fold and 6.2-fold higher deposition of LOR in the SC and stripped skin compared to LOR-Gel. For LORNE10, the amounts of LOR increased in SC and stripped skin by 2.3- and 5.5-fold, respectively, compared with the control. The rank of the skin retention improvement of LORNE was LORNE12 > LORNE11 > LORNE10 > LOR control.

Regarding the dermatocokinetic study, LORNE12-Gel was used due to its high skin retention. LOR retention in SC and stripped skin concentration profiles were determined (Fig. 7). Table 5 and Fig. 7 revealed that the results for $C_{Skin\ max}$ and $AUC_{0\text{-}48h}$ of SC and stripped skin treated with LORNE12-Gel are more significant compared to LOR-Gel ($p < 0.05$). LORNE12-Gel considerably enhanced LOR transference into the various layers of skin. When compared to the SC, the stripped skin layer showed a considerably higher AUC for LORNE12-Gel ($p < 0.05$).

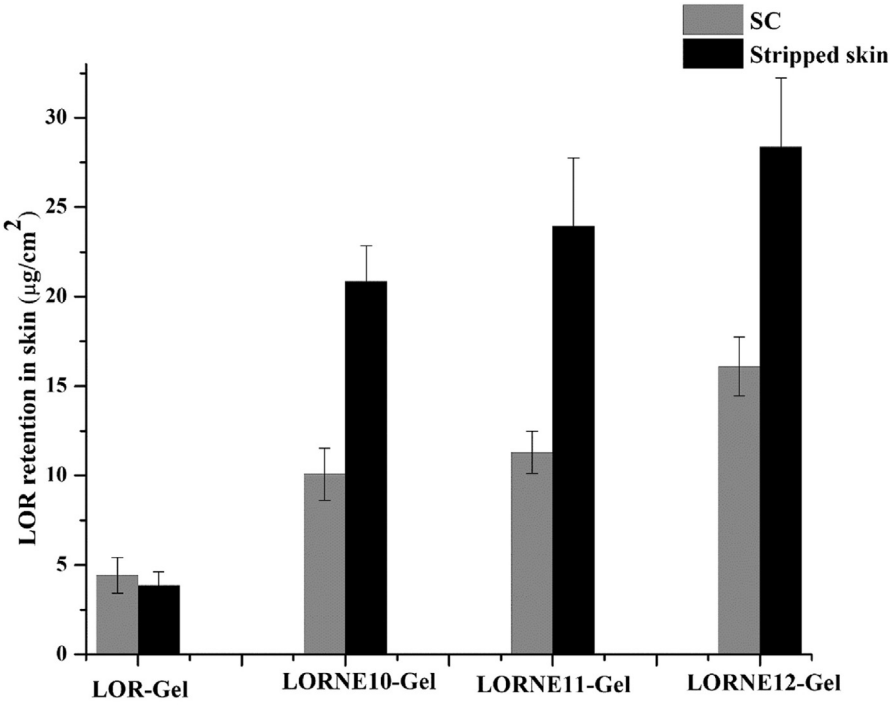


LORNE10 > LOR control.

**Fig. 6.** The amount of LOR retained in the SC and stripped skin after 48 h of topical application of LORNE10-Gel, LORNE11-Gel, LORNE12-Gel, and LOR-Gel.

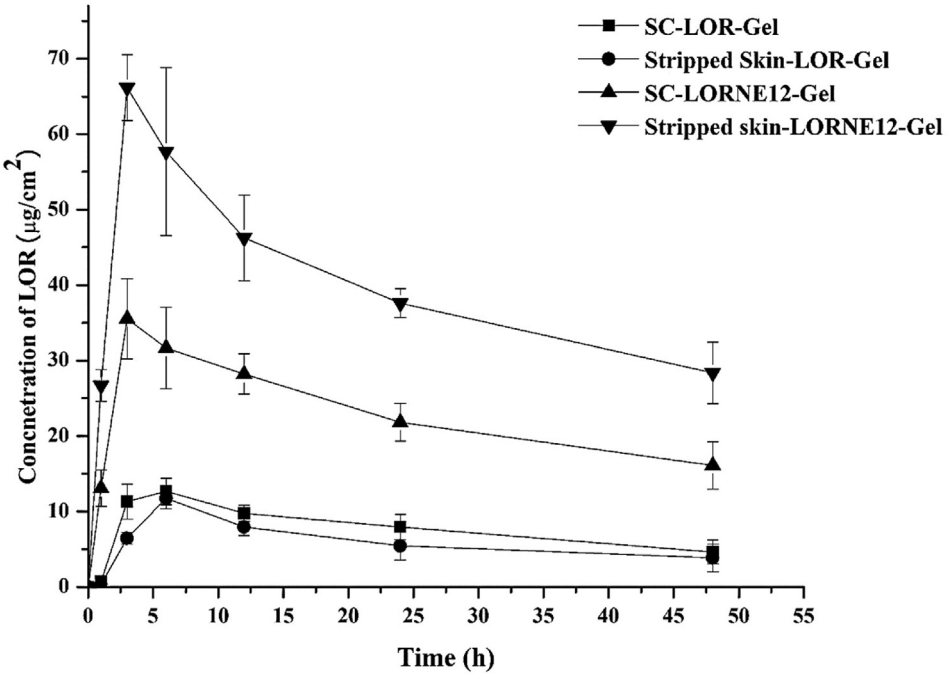


**Fig. 7.** Dermatokinetic profile of SC and stripped skin of LOR concentration (mean ± SD); n = 3.

*3.4.4. Anti-inflammatory studies of LORNE and LOR gels*

According to previous research, the carrageenan-induced paw edema rat model has been recognized as a reliable model for evaluating *in vivo* anti-inflammatory activities (Albrego et al., 2016). *The in vivo* performance of LORNE12-Gel was evaluated by measuring its anti-inflammatory activity in rats (Fig. 8). As depicted in Fig. 8, the % edema in nontreated animals (control) appeared to be increased after treatment with carrageenan alone for 8 h. However, the edema percentage in other groups was significantly decreased with the application of PBZ, LOR-Gel, and LORNE12-Gel. LORNE12-Gel markedly showed significant inhibition of edema at 3 h. LORNE12-Gel showed 33.1% inhibition of rat paw edema, which was significantly higher than LORNE12-Gel (15.3%) after 3 h compared to the control. These results correlate well with

**Table 5**
Pharmacokinetic parameters of LOR-Gel and LORNE12-Gel.

| Dermatokinetic parameters | LOR-Gel | | LORNE12-Gel | |
|---|---|---|---|---|
| | SC | Stripped skin | SC | Stripped skin |
| $C_{Skin\ max}$ (μg/cm$^2$) | 11.74 ± 2.34 | 12.68 ± 2.63 | 32.15 ± 5.68 | 67.43 ± 4.37 |
| $T_{Skin\ max}$ (h) | 6 | 6 | 3 | 3 |
| $AUC_{0\text{-}48h}$(μgcm$^{-2}$h) | 387.42 ± 45.65 | 278.52 ± 31.91 | 1105.34 ± 45.83 | 1902.78 ± 81.76 |
| $AUC_{0\text{-}\infty h}$(μg cm$^{-2}$h) | 581.11 ± 49.81 | 335.25 ± 48.12 | 1260.92 ± 82.27 | 3060.97 ± 21.15 |
| Ke(h$^{-1}$) | 1.51 ± 0.19 | 2.68 ± 0.36 | 0.49 ± 0.12 | 0.293 ± 0.04 |

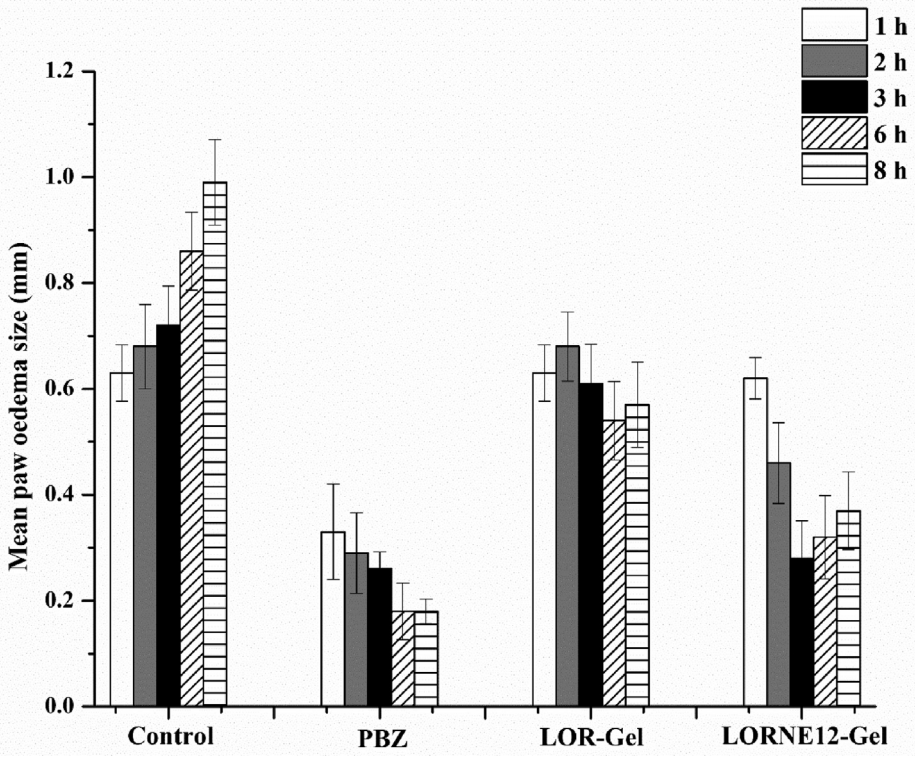


**Fig. 8.** Anti-inflammatory activity of control, PBZ, LOR-Gel, and LORNE12-Gel.

results obtained by *ex vivo* skin permeation and retention studies. PBZ significantly inhibited edema more than LOR-Gel and LORNE12-Gel during the experiment (Fig. 8).

*3.4.5. Skin irritation study of selected LORNE and LOR gels*

The skin irritation test was performed to confirm the safety of LORNE12-Gel following its transdermal administration. The irritation effect was documented for any visual signs of erythema. The topical application of LORNE12-Gel and LOR-Gel did not show any noticeable irritation during the time of the study (8 h) (Fig. 9). There was no erythema or redness observed on the skin after using the negative control group. However, the positive control presented significant erythema and redness. According to this visual outcome, LORNE12-Gel was free from any skin irritation and safe for transdermal drug delivery.

## 4. Discussion

The research for the treatment of inflammation is an important area of study in the medical field. Inflammation is associated with a wide range of diseases, and finding effective treatments can significantly improve patient outcomes. LOR NSAIDS oxicam is a strong anti-inflammatory drug used for pain management. But the available research precludes the use of LOR for long-term inflammation control due to its oral serious side effects. Transdermal delivery carriers are therefore desired to prevent LOR toxicity. Thus, nanocarriers could increase the therapeutic efficacy of LOR and decrease adverse effects. Topical use of SNEDDS can improve the effectiveness and reduce side effects of loaded LOR by enhancing its solubility and permeability through the skin. To develop effective SNEDDS formulations containing LOR, they must have sufficient solubility in various excipients (Badran et al., 2014, Zafar et al., 2021). Increased LOR solubility may enable the maximum amount of drug loading in SNEDDS without precipitation (Xue et al., 2018). Labrafil M 2125 CS as the oil phase is characterized by mono-, di- and triglycerides and PEG-6 mono- and diesters of the linoleic acid mixture. Hence, the solubility studies showed that Labrafil M 2125 CS has maximum solubility of LOR. The highest solubility of Cremophor RH40 as a surfactant may be attributed to the change in the lipophilic moiety of hydrogenated castor oil induced by condensation with polyethylene (Hamza and Aburahman, 2009). Furthermore, Cremophor EL and Cremophor ELP showed decreased solubility of LOR due to their low HLB values compared to Cremophor RH 40 (Hamza, and Aburahman, 2009). The solubility of LOR in the different aqueous solutions of Tweens depends on their degree of ethoxylation (Zhang et al., 2012). The importance of surfactants in the preparation of SNEDDSs is based on the reduction of interfacial tension promoting

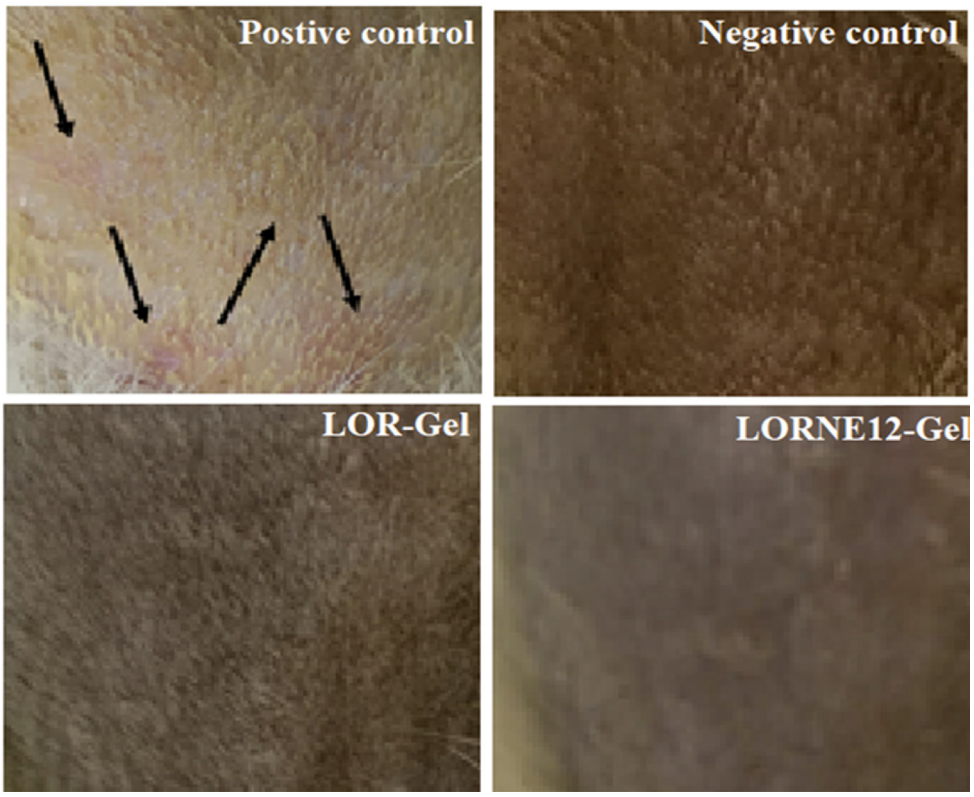


**Fig. 9.** Macroscopic images of skin treated with the positive control, negative control, LOR-Gel, and LORNE12-Gel.

spontaneous emulsification with low free energy (Patel et al., 2009). However, the interfacial tension may not be sufficiently reduced by surfactants alone (Buya et al., 2020). Hence, it is essential to use cosurfactants during the preparation of SNEDDSs to facilitate the homogeneity and stability of nanoemulsions (Li et al., 2015). Thus, Transcutol HP was selected as a cosurfactant due to its high solubility and miscibility with oil and water phases. It can easily disperse the oil phase into the water phase by further reducing the interfacial tension (Buya et al., 2020). It has been reported that Transcutol HP (cosurfactant) has a high ability to dissolve poorly water-soluble drugs such as clotrimazole and oridonin (Zhan et al., 2008, Borhade et al., 2012). Furthermore, ingredient selection for a SNEDDS is dependent on both solubility and HLB values, which are essential for the formation of a self-nanoemulsion (Subramaniam et al., 2017). Surfactants with HLB values of 12 to 15 are believed to have excellent spontaneous emulsification efficiency. The SNEDDS using a high HLB surfactant may keep the drug's solubilized state at the absorption site (Weerapol et al., 2014). Cremophor RH40 (high value of HLB, 15) and Transcutol HP (low value of HLB, 4.2) were effective surfactants/cosurfactants to provide successful self-nanoemulsifying formulations (Pouton et al., 2000). To identify the self-nanoemulsification region and an appropriate ratio of oil and $S_{mix}$ for the production of SNEDDS, ternary phase diagrams were constructed based on the solubility results (Parmar et al., 2011). A ternary diagram showed the nanoemulsion area with the proper concentration of Labrafil M 2125 CS, Cremophor RH40, and Transcutol HP for the preparation of SNEDDS. Accordingly, the $S_{mix}$ ratio (3:1) provides a more hydrophilic nature, which may form a good o/w nanoemulsion (Zhao et al., 2010). Furthermore, low $S_{mix}$ ratios exhibited a decrease in the nanoemulsion area, which may be attributed to the formation of a viscous liquid phase due to low surfactant concentration causing the spontaneous breakup of the oil–water interface (Wang et al., 2009). A higher $S_{mix}$ concentration is required to obtain smaller droplet sizes and stable formulations (Wang et al., 2009). This behavior is due to the reduction in interfacial tension and cohesion forces in the emulsion system (Wang et al., 2009). It has been reported that crystallization may or may not take place depending on a drug's solubility as opposed to its saturation system of SNEDDS (Narag et al., 2007). Therefore, the amount of LOR in the SNEDDS should be markedly lower than the saturated concentration of LOR in the SNEDDS. Otherwise, the high concentrations of the drug could increase at the oil/water interface of SNEDDS, causing decreased surfactant layer flexibility, and emulsification may be hindered by this interfacial particle layer (Wang et al., 2009). The emulsification time is the main key for confirming the spontaneity of self-nanoemulsions without the use of external heat or mechanical energy. The short self-emulsification time is based on the increased concentration of surfactant. Cremophor RH40 (surfactant) can reduce the interfacial tension between the aqueous and oil phases, producing a significant reduction in droplet size (Kallakunta et al., 2012). Additionally, Cremophor RH40 has a smaller packing parameter, which could be expected to impact the formation of fine droplets (Zhan et al., 2008). Therefore, LORNE formulations can be obtained with only gentle agitation due to the reduction in the interfacial free energy. The cosurfactants (Transcutol HP) can increase the interfacial fluidity by diffusing into the surfactant film, making void space between surfactant molecules (Constantinides and Scalert, 1997).

Nanoemulsion droplet size plays a very important role in improving drug absorption (Balakumar et al., 2013). The smaller droplet size of the emulsion resulted in a large interfacial surface area, which increased drug release and skin permeation of the drug (Ahmad et al., 2022). An increase in the concentration of surfactant may lead to high disruption of oil globules into smaller sizes, reducing droplet size (Shafiq et al., 2007). The reduction in droplet size can be attributed to the stabilization of oil droplets due to the presence of surfactant monolayers at the oil–water interface

(Shafiq et al., 2007; Ahmad et al., 2020). The incorporation of a cosurfactant may enlarge the monolayer film, causing smaller droplet diameters with a uniform size distribution (Fahmy et al., 2015). This reduction in droplet size may be attributed to the smaller packing parameter of Cremophor RH 40, which allows the most efficient packing of surfactant molecules upon association with water molecules, leading to the formation of fine droplets. It has been confirmed that nanoemulsions can be sterically stabilized by nonionic surfactants with low droplet charge (Tang et al., 2012). Moreover, nonionic surfactants may produce a negatively charged interface due to their ability to adsorb the hydroxyl ion ($OH^-$) and hydrated oxonium ion ($H_3O^+$), resulting in negative zeta-potential values of LORNE (Ahmad et al., 2022).

To predict the *in vivo* performance or to assess the behavior of drug release from the system, an *in vitro* drug release study is particularly important (Marín-Quintero et al., 2013). The *in vitro* release results reveal the contribution of the SNEDDS formulation in enhancing LOR solubilization and *in vitro* release. The self-emulsifying characterization of the excipients used for LORNE preparation may be responsible for the high drug release behavior. Furthermore, the drug molecules were also helped by these excipients to become solubilized micelles in the solution state, causing the formation of ultrafine droplets in the aqueous dispersion. Therefore, dissolution studies specifically assisted the role of excipients in enhancing the drug's state of dissolution. To formulate a transdermal delivery system, it is important to reduce the *lag* time in skin permeation and achieve an appropriate transdermal flux. LORNE10, LORNE11, and LORNE12 were used for the *ex vivo* permeation study due to their high LOR release.

For transdermal purposes, it is important to prolong the contact time between the drug and the skin surface, and carbopol 934, as a gel-forming polymer was used to increase the adhesion of LORNE to the skin surface. The LORNE-loaded hydrogels have acceptable characterization for transdermal performance. The improved transdermal permeability parameters (Jss and KP) of LORNE could be due to the presence of permeation enhancers such as Labrafil M 2125C, Cremophor, and Transcutol-HP. Due to its dilution with water from the epidermal layer, as well as water absorption and swelling carbopol gel, LORNE may have a considerable impact on the permeation properties of LOR. The skin may come into contact with the SNEDDS nanodroplets, producing a greater surface area for drug absorption (Badran et al., 2014). Due to SC swelling and hydration, the occlusive nature of SNEDDSs causes considerable LOR permeation (Badran et al., 2014). Additionally, moisture may disrupt the lipid bilayers of SC, resulting in significant skin permeability (Yuan et al., 2006). The fluidization of lipids in SC in the presence of surfactants and oil as SNEDDS components may change the SC's barrier properties and increase LOR permeability (Abd et al., 2016). In addition, the high skin retention and dermatokinetic parameters of LORNE12-Gel may be due to the high concentration of cremophor RH40, which can disrupt the SC (Soliman et al., 2010). LORNE12 showed the highest cumulative permeation, permeation flux, and skin layer uptake. This behavior may be attributed to the nanoemulsion composition and lowest droplet size. It is important to investigate the occlusivity by measuring the *trans*-epidermal water loss (TEWL) as an important factor for improved permeability for a mechanistic view in the future. The smallest droplets of LORNE 12 may well enhance the skin retention of the dug associated with an increased number of nanodroplets that can interact with SC (El-Say et al. 2015). The presence of surfactants in SNEDDS could fluidize the lipid bilayers of SC, improving the efficacy of LOR (El-Say et al. 2015). The outcomes demonstrated the superiority of the produced nanogel that reached LOR in the various skin layers for the treatment of inflammation (Shakeel et al., 2019). Hence, LORNE12-Gel could improve an anti-inflammatory outcome by strong edema inhibition compared to LOR-Gel due to the LORNE structure that promotes the skin permeation and retention of LOR (Altamimi et al., 2019). The gel formulation contained surfactants as a permeation enhancer that could facilitate rapid drug permeation, as observed by a decrease in rat paw edema (El-Say et al. 2016). Thus, these results suggest the superiority of LORNE12-Gel for the management of inflammation. This behavior could be attributed to the smaller droplet size of LORNE12. The results provided a possible and effective formulation (LORNE12-Gel) that can be used to manage inflammation.

## 5. Conclusions

The formed SNEDDS using Labrafil M2125 CS (oil phase), Cremophor RH40 (surfactant), and Transcutol-HP (cosurfactant) using a ternary phase diagram showed an appropriate region for the nanoemulsion. The $S_{mix}$ ratio of the selected self-nanoemulsion had a significant impact on the solubilization of LOR with a nanometer range and short emulsification time. *In vitro* drug release of LOR from selected SNEDDS (LORNE) formulations was higher than that of the LOR control. *Ex vivo* skin permeation/retention experiments showed that LORNE-Gels had a high level of LOR permeation in a controlled manner with significant retention amounts of LOR in skin layers. LORNE12-Gel showed enhanced permeation and skin retention of LOR. Further dermatokinetic study revealed better retention of LORNE12-Gel than LOR-Gel in SC and stripped skin layers. Furthermore, LORNE12-Gel showed promising therapeutic efficacy (*in vivo* anti-inflammatory activity) compared with LOR-Gel. The skin irritation study revealed that LORNE12-Gel had no irritation. The obtained data suggest that LORNE12-Gel might be explored for the transdermal delivery of LOR with improved skin retention and anti-inflammatory efficacy.

## Declaration of Competing Interest

The authors declare that they have no known competing financial interests or personal relationships that could have appeared to influence the work reported in this paper.

## Acknowledgments

The authors would like to extend their sincere appreciation to the Researchers Supporting Project Number (RSP2023R301), King Saud University, Riyadh, Saudi Arabia.

## References

Abd, E., Namjoshi, S., Mohammed, Y.H., Roberts, M.S., Grice, J.E., 2016. Synergistic skin penetration enhancer and nanoemulsion formulations promote the human epidermal permeation of caffeine and naproxen. J. Pharm. Sci. 105 (1), 2121–2210.

Ahmad, N., Rizwan, A., Taysser, M.B., Hussain, S.A., Hassan, A.A., 2020. A comparative ex vivo permeation evaluation of a novel 5-Fluorocuracil nanoemulsion-gel by topically applied in the different excised rat, goat, and cow skin. Saudi J. Biol. Sci. 27 (4), 1024–1040.

Ahmad, N., Ahmed, A.A., Mohd, F.K., Zabih, U., Taysser, M.B., et al., 2022. A novel 5-Fluorocuracil multiple-nanoemulsion used for the enhancement of oral bioavailability in the treatment of colorectal cancer. Saudi J. Biol. Sci. 29 (5), 3704–3716.

Ahmed, O.A., Afouna, M.I., El-Say, K.M., Abdel-Naim, A.B., Khedr, A., Banjar, Z.M., 2014. Optimization of self-nanoemulsifying systems for the enhancement of *in vivo* hypoglycemic efficacy of glimepiride transdermal patches. Expert Opin. Drug Deliv. 11, 1005–1013.

Al-Suwayeh, S..A, Taha, E.I., Al-Qahtani, F.M., Ahmed, M.O., Badran, M.M., 2014. Evaluation of skin permeation and analgesic activity effects of carbopol lornoxicam topical gels containing penetration enhancer. Scientific World Journal 2014, 127495. https://doi.org/10.1155/2014/127495.

Altamimi, M.A., Kazi, M., Hadi, A.M., Ahad, A., Raish, M., 2019. Development and optimization of self-nanoemulsifying drug delivery systems (SNEDDS) for

curcumin transdermal delivery: an anti-inflammatory exposure. Drug Dev. Ind. Pharm. 45 (7), 1073–1078.
Altamimi, M., Nazrul, H., Sultan, A., Wajhul, Q., Shakeel, F., 2019. Enhanced Skin Permeation of Hydrocortisone Using Nanoemulsion as Potential Vehicle. Chemistry Select 13 (34), 10084–10091.
Badran, M.M., Taha, E.I., Tayel, M.M., Al-Suwayeh, S.A., 2014. Ultrafine self-nanoemulsifying drug delivery system for transdermal delivery of meloxicam: dependency on the type of surfactants. J. Mol. Liquids. 190, 16–22.
Balakumar, K., Raghavan, C.V., Abdu, S., 2013. Self-nanoemulsifying drug delivery system (SNEDDS) of rosuvastatin calcium: design, formulation, bioavailability and pharmacokinetic evaluation. Colloids Surf. B: Biointerfaces. 112, 337–343.
Beg, S., Swain, S., Singh, H.P., Patra, C.N., Rao, M.B., 2012. Development, optimization, and characterization of solid self-nanoemulsifying drug delivery systems of valsartan using porous carriers. AAPS PharmSciTech. 13 (4), 1416–1427.
Borhade, V., Pathak, S., Sharma, S., Patravale, V., 2012. Clotrimazole nanoemulsion for malaria chemotherapy. Part I: Preformulation studies, formulation design and physicochemical evaluation. Int. J. Pharm. 431 (1–2), 138–148.
Buya, A.B., Ucakar, B., Beloqui, A., Memvanga, P.B., Préat, V., 2020. Design and evaluation of self-nanoemulsifying drug delivery systems (SNEDDSs) for senicapoc. Int. J. Pharm. 30, (580) 119180.
Chen, M.X., Alexander, K., Baki, G., 2016. Formulation and evaluation of antibacterial creams and gels containing metal ions for topical application. J. Pharm. 2016, 5754349.
Constantinides, P.P., Scalart, P., 1997. Formulation and physical characterization of water-in-oil microemulsions containing long-versus medium-chain glycerides. Int. J. Pharm. 158 (1), 57–68.
El-Megrab, N.A., El-Nahas, H.M., Balata, G.F., 2006. Formulation and evaluation of meloxicam gels for topical administration. Saudi Pharm J. 14 (3/4), 155.
Elmowafy, M., Khaled, S., Hazim, M.A., Nabil, K.A., Ayman, S., Mohamed, F.I., Mohamed, A.A., Tarek, A.A., 2019. Impact of nanostructured lipid carriers on dapsone delivery to the skin: *in vitro* and *in vivo* studies. Int. J. Pharm. 572, 118781.
El-Say, K.M., Abd-Allah, F.I., Lila, A.E., Hassan, A.S., Kassem, A.E., 2016. Diacerein niosomal gel for topical delivery: development, in vitro and in vivo assessment. J. Liposome Res. 26 (1), 57–68.
El-Say, K.M., Ahmed, T.A., Badr-Eldin, S.M., Fahmy, U., Aldawsari, H., Ahmed, O.A., 2015. Enhanced permeation parameters of optimized nanostructured simvastatin transdermal films: ex vivo and in vivo evaluation. Pharm. Dev. Technol. 20 (8), 919–926.
Fahmy, U.A., Ahmed, O.A., Hosny, K.M., 2015. Development and evaluation of avanafil self-nanoemulsifying drug delivery system with rapid onset of action and enhanced bioavailability.". AAPS PharmSciTech. 16 (1), 53–58.
Gursoy, R.N., Benita, S., 2004. Self-emulsifying drug delivery systems (SEDDS) for improved oral delivery of lipophilic drugs. Biomed. Pharmacother. 58 (3), 173–182.
Hamza, Y.-E.-S., Aburahman, M.H., 2009. Design and *in vitro* evaluation of novel sustained-release double-layer tablets of lornoxicam: utility of cyclodextrin and xanthan gum combination. AAPS Pharm SciTech. 10 (4), 1357.
Helmy, H.S., El-Sahar, A.E., Sayed, R.H., Shamma, R.N., Salama, A.H., Elbaz, E.M., 2017. Therapeutic effects of lornoxicam-loaded nanomicellar formula in experimental models of rheumatoid arthritis. Int. J. Nanomedicine. 22 (12), 701–7023.Hesham, M.T., Ahmed, A.H., Jelan, A.A., Yasser, A.H., Dina, F., 2020. Transfersomal gel nanocarriers for enhancement the permeation of lornoxicam. J. Drug Deliv. Sci. Technol. 56. Part A 101540, 1773–2247.
Hesham, M.T., Ahmed, A.H.A., Jelan, A.A., Yasser, A.H., Dina, F., 2020. Transfersomal gel nanocarriers for enhancement the permeation of lornoxicam. J. Drug Deliv. Sci. Technol. 56, 1773–2247.
Heshmati, N., Cheng, X., Eisenbrand, G., Fricker, G., 2013. Enhancement of oral bioavailability of E804 by self-nanoemulsifying drug delivery system (SNEDDS) in rats. J. Pharm. Sci. 102 (10), 3792–3799.
Isola, G., Polizzi, A., Iorio-Siciliano, V., et al., 2021. Effectiveness of a nutraceutical agent in the non-surgical periodontal therapy: a randomized, controlled clinical trial. Clin. Oral Invest. 25, 1035–1045.
Kallakunta, V.R., Bandari, S., Jukanti, R., Veerareddy, P.R., 2021. Oral self-emulsifying powder of lercanidipine hydrochloride: formulation and evaluation. Powder Technol. 221, 375–382.
Kavitha, K., Rajendra, M.M., 2011. Design and evaluation of transdermal films of lornoxicam. Int. J. Pharm. Bio. Sci. 2 (2), 54–62.
Kohli, K., Chopra, S., Dhar, D., Arora, S., Khar, R.K., 2010. Self-emulsifying drug delivery systems: an approach to enhance oral bioavailability. Drug discovery today. 15 (21–22), 958–965.
Lala, R., Awari, N., 2014. Nanoemulsion-based gel formulations of COX-2 inhibitors for enhanced efficacy in inflammatory conditions. Appl. Nanosci. 4 (2), 143–151.
Lapasin, R., Grassi, M., Coceani, N., 2001. Effects of polymer addition on the rheology of o/w microemulsions. Rheologica Acta. 40 (2), 185–192.
Li, F., Song, S., Guo, Y., Zhao, Q., Zhang, X., Pan, W., Yang, X., 2015. Preparation and pharmacokinetics evaluation of oral self-emulsifying system for poorly water-soluble drug Lornoxicam. Drug Deliv 22 (4), 487–498.
Londhe, V., Thakkar, V., Ranade, S., 2013. Topical delivery of lornoxicam: design, evaluation and effect of penetration enhancers. Indo. American J. Pharm. Res. 3, 3174–3181.
Marín-Quintero, D., Fernandez-Campos, F., Calpena-Campmany, A.C., et al., 2013. Formulation design and optimization to improve nystatin-loaded lipid intravenous emulsions. J. Pharm. Sci. 102 (11), 4015–4023.
Narahari, N., Das, M., 2005. Lornoxicam loaded solid lipid nanoparticles for topical delivery: ex vivo assessment and pharmacodynamics activity. World J. Pharm. Sci. 3 (5), 862–871.
Narang, A.S., Delmarre, D., Gao, D., 2007. Stable drug encapsulation in micelles and microemulsions. Int. J. Pharm. 345 (1–2), 9–25.
Parmar, N., Singla, N., Amin, S., Kohli, K., 2011. Study of cosurfactant effect on nanoemulsifying area and development of lercanidipine loaded (SNEDDS) self-nanoemulsifying drug delivery system. Colloids Surf. B: Biointerfaces. 86 (2), 327–338.
Patel, D., Sawant, K.K., 2009. Self-microemulsifying drug delivery system: formulation development and biopharmaceutical evaluation of lipophilic drugs. Current drug Deliv. 6 (4), 419–424.
Pouton, C.W., 2000. Lipid formulations for oral administration of drugs: nonemulsifying, self-emulsifying and self-microemulsifying drug delivery systems. Eur. J. Pharm. Sci. 11, S93–S98.
Radhofer-Welte, S., Rabasseda, X., 2000. Lornoxicam, a new potent NSAID with an improved tolerability profile. Drugs Today (Barc) 36 (1), 55–76.
Rai, V.K., Mishra, N., Yadav, K.S., Yadav, N.P., 2018. Nanoemulsion as pharmaceutical carrier for dermal and transdermal drug delivery: Formulation development, stability issues, basic considerations and applications. J. control. release. 270, 203–225.
Rapalli, V.K., Swati, S., Aniruddha, R., Gautam, S., 2021. Design and dermatokinetic evaluation of Apremilast loaded nanostructured lipid carriers embedded gel for topical delivery: A potential approach for improved permeation and prolong skin deposition. Colloids and Surfaces B: Biointerfaces 206, 0927–7765.
Razzaq, F.A., Muhammad, A., Sajid, A., et al., 2021. Glimepiride-Loaded Nanoemulsion, Development, *In Vitro* Characterization, *Ex Vivo* Permeation and *In Vivo* Antidiabetic Evaluation. Cells. 10 (9), 2404. https://doi.org/10.3390/cells10092404.
Rizwan, M., Aqil, M., Azeem, A., Talegaonkar, S., Sultana, Y., Ali, A., 2010. Enhanced transdermal delivery of carvedilol using nanoemulsion as a vehicle. J. Expert. Nanosci. 5 (5), 390–411.
Shafiq, S., Shakeel, F., Talegaonkar, S., et al., 2007. Formulation development and optimization using nanoemulsion technique: a technical note. AAPS pharmscitech. 8 (2), E12–E17.
Shakeel, F., Haq, N., Alanazi, F.K., Alsarra, I.A., 2014. Polymeric solid self-nanoemulsifying drug delivery system of glibenclamide using coffee husk as a low cost biosorbent. Powder Technol. 256, 352–360.
Shakeel, F., Alam, P., Anwer, M.K., Alanazi, S.A., Alsarra, I.A., Alqarni, M.H., 2019. Wound healing evaluation of self-nanoemulsifying drug delivery system containing Piper cubeba essential oil. 3 Biotech 9, 82.
Soliman, S.M., Malak, N.A., El-Gazayerly, O.N., Rehim, A.A., 2010. Formulation of microemulsion gel systems for transdermal delivery of celecoxib: *In vitro* permeation, anti-inflammatory activity and skin irritation tests. Drug Discov. Ther. 4 (6), 459–471.
Subramaniam, P., Siddalingam, R., 2017. Self-nanoemulsifying drug delivery systems of poorly soluble drug dutasteride: formulation and *in vitro* characterization. J. App. Pharm. Sci. 7, 11–22.
Taha, E.I., Al-Suwayeh, S.A., Mahrous, G.M., 2018. Simple, fast and reliable reversed-phase HPLC method for lornoxicam analysis in pharmaceutical formulations. World J. Pharm. Res. 8, 28–35.
Tang, S.Y., Manickam, S., Wei, T.K., Nashiru, U.S., 2012. Formulation development and optimization of a novel Cremophore EL-based nanoemulsion using ultrasound cavitation. Ultrason Sonochem. 19 (2), 330–345.
Ueda, C.T., Shah, V.P., Derdzinski, K., Ewing, G., et al., 2009. Topical and transdermal drug products. Pharmacopeial Forum. 35 (3), 750–764.
Wada, Y., Etoh, Y., Ohira, A., Kimata, H., Koide, T., Ishihama, H., Mizushima, Y., 1982. Percutaneous absorption and anti-inflammatory activity of indomethacin in ointment. J. Pharm. Pharmacol. 34 (7), 467–468.
Wang, L., Dong, J., Chen, J., Eastoe, J., Li, X., 2009. Design and optimization of a new self-nanoemulsifying drug delivery system. J. Colloid Interface sci. 330 (2), 443–448.
Weerapol, Y., Limmatvapirat, S., Nunthanid, J., Sriamornsak, P., 2014. Self-nanoemulsifying drug delivery system of nifedipine: impact of hydrophilic-lipophilic balance and molecular structure of mixed surfactants. AAPS PharmSciTech. 15, 456–464.
Xue, X., Cao, M., Ren, L., Qian, Y., Chen, G., 2018. Preparation and optimization of rivaroxaban by self-nanoemulsifying drug delivery system (SNEDDS) for enhanced oral bioavailability and no food effect. AAPS PharmSciTech. 19 (4), 1847–1859.
Yuan, Y., Li, S.-M., Mo, F.-K., Zhong, D.-F., 2006. Investigation of microemulsion system for transdermal delivery of meloxicam. Int. J. Pharm. 321 (1–2), 117–123.
Zafar, A., Imam, S.S., Alruwaili, N.K., et al., 2021. Development of piperine-loaded solid self-nanoemulsifying drug delivery system: optimization, *In Vitro*, Ex Vivo, and *In Vivo* Evaluation. Nanomaterials 11 (11), 2920.
Zhan, P., Liu, Y., Feng, N., Xu, J., 2008. Preparation and evaluation of self-microemulsifying drug delivery system of oridonin. Inter. J. Pharm. 355 (1–2), 269–276.

Zhang, R., Wang, Y., Tan, L., Zhang, H., Yang, M., 2012. Analysis of polysorbate 80 and its related compounds by RP-HPLC with ELSD and MS detection. J. Chromat. Sci. 50 (7), 598–607.
Zhao, X., Liu, J., Zhang, X., Li, Y., 2006. Enhancement of transdermal delivery of theophylline using microemulsion vehicle. Int. J. Pharm. 327 (1–2), 58–64.
Zhao, Y., Wang, C., Chow, A.H., et al., 2010. Self-nanoemulsifying drug delivery system (SNEDDS) for oral delivery of Zedoary essential oil: formulation and bioavailability studies. Int. J. Pharm. 383 (1–2), 170–177.
Zheng, Y., Ouyang, W.-Q., Wei, Y.-P., Syed, S.-F., et al., 2016. The effects of carbopol® 934 proportion on nanoemulsion gel for topical and transdermal drug delivery: a skin permeation study. Inter. J. Nanomedicine. 11, 5971.